



# Synthesis of covalently linked linear porphyrin triad and tetrad containing different porphyrin sub-units

S. Punidha, M. Ravikanth\*

Department of Chemistry, Indian Institute of Technology, Powai, Mumbai 400076, India

## ARTICLE INFO

### Article history:

Received 26 February 2008

Received in revised form 7 May 2008

Accepted 7 May 2008

Available online 11 May 2008

### Keywords:

Porphyrin arrays

Functionalized porphyrins

Weak interaction

Energy transfer

## ABSTRACT

Covalently linked diarylethyne bridged unsymmetrical porphyrin triad containing ZnN<sub>4</sub>, N<sub>4</sub>, and N<sub>2</sub>S<sub>2</sub> porphyrin sub-units and porphyrin tetrad containing ZnN<sub>4</sub>, N<sub>4</sub>, N<sub>3</sub>S, and N<sub>2</sub>S<sub>2</sub> porphyrin sub-units were synthesized over sequence of Pd(0) mediated coupling reactions. The triad and tetrad are freely soluble in all common organic solvents and characterized by ES-MS, NMR, absorption, fluorescence, and electrochemical techniques. The <sup>1</sup>H NMR, absorption, and electrochemical studies indicated a weak interaction between the porphyrin sub-units of porphyrin triad and porphyrin tetrad. The steady state and time-resolved fluorescence studies supported an energy transfer from one end of porphyrin array to the other end. This kind of porphyrin arrays containing different porphyrin sub-units will be useful for molecular electronics applications.

© 2008 Elsevier Ltd. All rights reserved.

## 1. Introduction

The syntheses of photosynthetic and related model systems require methods for joining large numbers of porphyrins into functional arrays. One modular approach employs porphyrin building blocks bearing peripheral functional groups that can be joined via specific coupling methods to generate porphyrin assemblies.<sup>1</sup> The porphyrin assemblies are of fundamental importance as attractive building blocks for the modular construction of electronics, optical devices, sensors, and solar energy conversions.<sup>2–6</sup> A number of covalently linked porphyrin arrays have been developed with the aim of reproducing and understanding light-harvesting and charge-separation phenomena in photosynthetic organisms in addition to their potential use in molecular device applications. In this approach the inter-porphyrin linker is formed concomitantly with the joining step, thus the nature of the linker and the coupling method are closely intertwined. Among the various linkers that have been explored, ethynes, butadiynes, or polynes have many attractive design features.<sup>2–6</sup> Arrays comprised of weakly coupled pigments are ideally suited for energy transfer modeling, as the energy transfer process occurs without significant alteration of the remaining excited state photophysical processes.<sup>7–10</sup> The diarylethyne linked multiporphyrin arrays are weakly coupled electronically. In diarylethyne bridged multiporphyrin arrays the absorption spectra of the arrays are essentially a composite of the

individual porphyrin spectra, indicating limited excitonic interaction. The weak electronic coupling and the efficient energy transfer properties of these arrays make them well suited for modeling.<sup>7–10</sup> Diarylethyne linked arrays have been constructed by the Pd catalyzed cross-coupling reaction of a porphyrin arylidide and a porphyrin arylethyne.<sup>11</sup> This building block approach is quite versatile and has yielded energy funnels,<sup>12</sup> molecular wires,<sup>13,14</sup> and opto-electronic gates.<sup>15</sup> Rapid and efficient photoinduced energy transfer among the porphyrins was observed in each of these architectures. The reports available till date in literature on diarylethyne porphyrin assemblies used ZnN<sub>4</sub> porphyrin sub-unit as donor at one end and N<sub>4</sub> porphyrin sub-unit as acceptor at another end.<sup>13–15</sup> It has been observed that these assemblies transfer excited singlet-state energy from one end to the other very efficiently. Recently, we synthesized several covalently linked diarylethyne bridged unsymmetrical porphyrin dyads<sup>16–21</sup> containing two different porphyrin cores such as N<sub>4</sub>–N<sub>3</sub>O, N<sub>4</sub>–N<sub>3</sub>S, N<sub>3</sub>O–N<sub>3</sub>S, N<sub>3</sub>S–N<sub>2</sub>S<sub>2</sub>, etc. In these dyads, the energy gradient was created in their metal free form since the two porphyrin sub-units in dyads are two different macrocycles having different singlet-state energies hence useful to study singlet–singlet energy transfer from one unit to the other. A sequential array of porphyrins containing three or more different porphyrin sub-units would help us to understand the designing principles for opto-electronic device applications. Thus, in continuation of our efforts toward synthesizing unsymmetrical porphyrin arrays containing different porphyrin sub-units, in this paper, we describe the synthesis of covalently linked diarylethyne bridged unsymmetrical linear porphyrin triad **1** containing three different porphyrin sub-units such as ZnN<sub>4</sub>, N<sub>4</sub>, and N<sub>2</sub>S<sub>2</sub> porphyrin

\* Corresponding author. Tel.: +91 22 5767176; fax: +91 22 5723480.

E-mail address: [ravikanth@chem.iitb.ac.in](mailto:ravikanth@chem.iitb.ac.in) (M. Ravikanth).

sub-units and diarylethynyl bridged unsymmetrical linear porphyrin tetrad **2** containing four different porphyrin sub-units such as ZnN<sub>4</sub>, N<sub>4</sub>, N<sub>3</sub>S, and N<sub>2</sub>S<sub>2</sub> porphyrin sub-units (Chart 1). The porphyrin triad and tetrad were characterized by NMR, mass, absorption, fluorescence, and electrochemical methods. The preliminary fluorescence studies supported an efficient energy transfer from one end of porphyrin array to the other end.

## 2. Results and discussion

The porphyrin building blocks required for synthesis of porphyrin triad **1** and tetrad **2** are shown in Chart 2. The trans di-functionalized N<sub>4</sub> **3** and N<sub>3</sub>S **4** porphyrin building blocks possessing *meso*-iodophenyl and *meso*-ethynylphenyl functional groups that provide versatile handles for incorporation into a variety of architectures was prepared by following the literature reported methods.<sup>22</sup> The mono-functionalized ZnN<sub>4</sub> porphyrin<sup>23</sup> **5** and N<sub>2</sub>S<sub>2</sub> porphyrin<sup>17</sup> **6** building blocks containing one ethynylphenyl and one iodophenyl group, respectively, were prepared as reported in the literature.

### 2.1. Synthesis of covalently linked linear ZnN<sub>4</sub>–N<sub>4</sub>–N<sub>2</sub>S<sub>2</sub> porphyrin triad (**1**)

The linear porphyrin triad containing ZnN<sub>4</sub>, N<sub>4</sub>, and N<sub>2</sub>S<sub>2</sub> porphyrin sub-units is synthesized over sequence of steps as shown in Scheme 1. In the first step, the ZnN<sub>4</sub>–N<sub>4</sub> porphyrin dyad **7** was synthesized under Lindsey's copper free Pd(0) coupling conditions<sup>11</sup> by coupling of **5** and **3** in toluene/triethylamine at 35 °C in the presence of a catalytic amount of Pd<sub>2</sub>(dba)<sub>3</sub>/AsPh<sub>3</sub> (Scheme 1).<sup>24</sup> The progress of the reaction was monitored with TLC and absorption spectroscopy. After standard work-up, the crude reaction mixture was subjected to silica gel column chromatography and the pure porphyrin dyad **7** was obtained in 55% yield as purple solid. The dyad **7** was characterized by all spectroscopic techniques. The ES-MS spectrum showed a peak at 1480.3 corresponding to [M<sup>+</sup>–H] confirming the dyad **7**. The resonances of <sup>1</sup>H NMR spectrum of dyad **7** was assigned on the basis of the spectra observed for the corresponding two monomers taken independently. In ZnN<sub>4</sub>–N<sub>4</sub> porphyrin dyad **7**, the 16 pyrrole protons, 8 belonging to ZnN<sub>4</sub> porphyrin sub-unit and 8 belonging to N<sub>4</sub> porphyrin sub-unit

appeared as a multiplet in the region of  $\delta$ =8.78–9.00 ppm. The trimethylsilyl protons appeared as a singlet at  $\delta$ =0.38 ppm. A comparison of chemical shifts of the various protons of dyad **7** with those of corresponding individual monomeric porphyrin units indicates only minor differences suggesting that the two porphyrin sub-units in the dyad interact very weakly. The ZnN<sub>4</sub>–N<sub>4</sub> porphyrin dyad **8** having a free phenylethynyl group at the *meso*-position of N<sub>4</sub> porphyrin sub-unit necessary for further coupling was obtained in the next step by refluxing the dyad **7** with K<sub>2</sub>CO<sub>3</sub> in THF/CH<sub>3</sub>OH at 60 °C<sup>23</sup> for 6 h followed by purification on silica gel column. The dyad **8** was characterized by all spectroscopic techniques. The ES-MS spectrum showed a peak at 1408.3 corresponding to [M<sup>+</sup>–H] confirming the dyad **8** (Fig. 1a). The <sup>1</sup>H NMR spectrum of dyad **8** showed the disappearance of signal at  $\delta$  0.38 ppm corresponding to trimethylsilyl protons and the appearance of signal at  $\delta$  3.33 ppm corresponding to ethynyl proton confirmed the dyad **8** (Fig. 2a).

In the next step, the ZnN<sub>4</sub>–N<sub>4</sub>–N<sub>2</sub>S<sub>2</sub> triad **1** was prepared by coupling of **6** and **8** under identical palladium coupling conditions used for dyad **7** (Scheme 1).<sup>11</sup> The triad reaction worked smoothly and required two silica gel column chromatographic purifications. The triad **1** was obtained in 45% yield and was confirmed by ES-MS spectrum shown in Figure 1b. In the <sup>1</sup>H NMR spectrum of ZnN<sub>4</sub>–N<sub>3</sub>S–N<sub>2</sub>S<sub>2</sub> triad **1** (Fig. 2b), the resonances corresponding to all three porphyrinic sub-units and the bridging groups are present. The four  $\beta$ -thiophene protons of N<sub>2</sub>S<sub>2</sub> porphyrin sub-unit appeared as two sets of resonances in  $\delta$  9.62–9.72 ppm region. The 20 pyrrole protons, 4 belonging to N<sub>2</sub>S<sub>2</sub> porphyrin sub-unit, 8 belonging to N<sub>4</sub> porphyrin sub-unit, and 8 belonging to ZnN<sub>4</sub> porphyrin sub-unit appeared as sets of overlapping signals in  $\delta$  8.62–8.98 ppm region (Fig. 2b). The NH protons of N<sub>4</sub> porphyrin sub-unit appeared as a broad singlet at  $\delta$  –2.76 ppm.

### 2.2. Synthesis of covalently linked linear ZnN<sub>4</sub>–N<sub>4</sub>–N<sub>3</sub>S–N<sub>2</sub>S<sub>2</sub> porphyrin tetrad (**2**)

The synthesis of linear porphyrin tetrad **2** containing four different porphyrin sub-units ZnN<sub>4</sub>–N<sub>4</sub>–N<sub>3</sub>S–N<sub>2</sub>S<sub>2</sub> porphyrins with a progressive decrease in energy levels (Scheme 2) involves the following steps: (1) synthesis of linear dyad having ZnN<sub>4</sub> and N<sub>4</sub> porphyrin sub-units having one *meso*-phenylethynyl group on N<sub>4</sub> porphyrin sub-unit, (2) synthesis of linear triad having ZnN<sub>4</sub>, N<sub>4</sub>, and

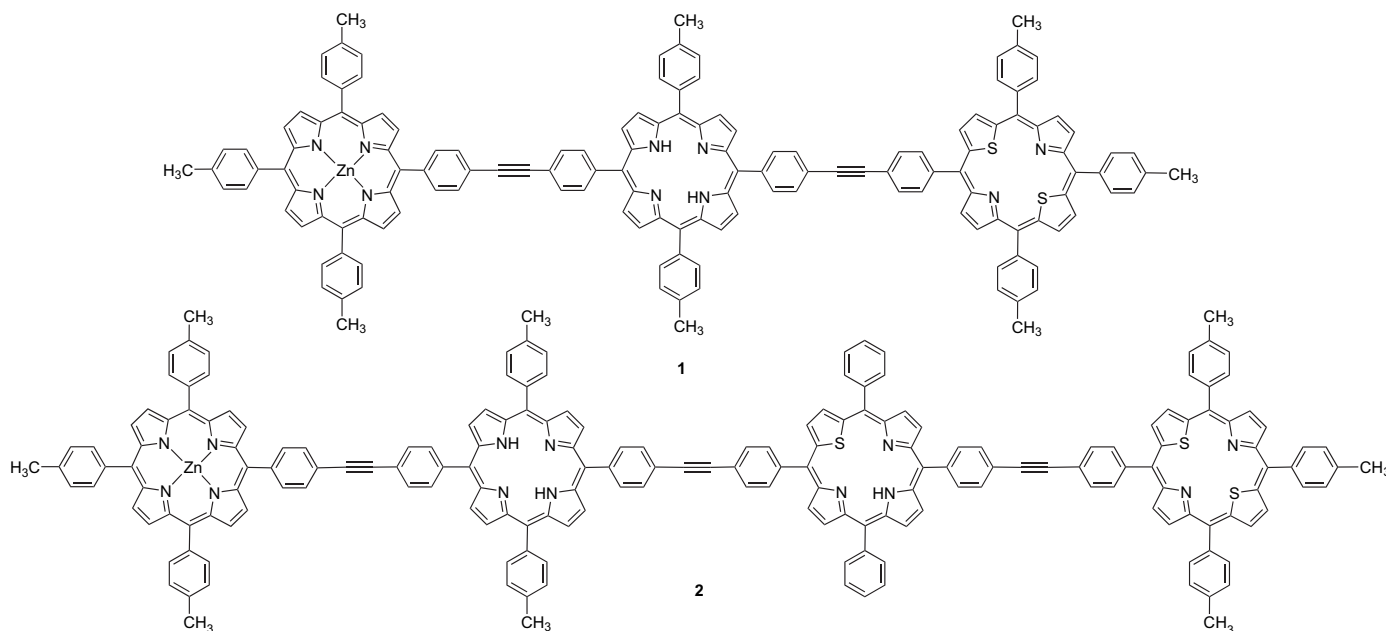
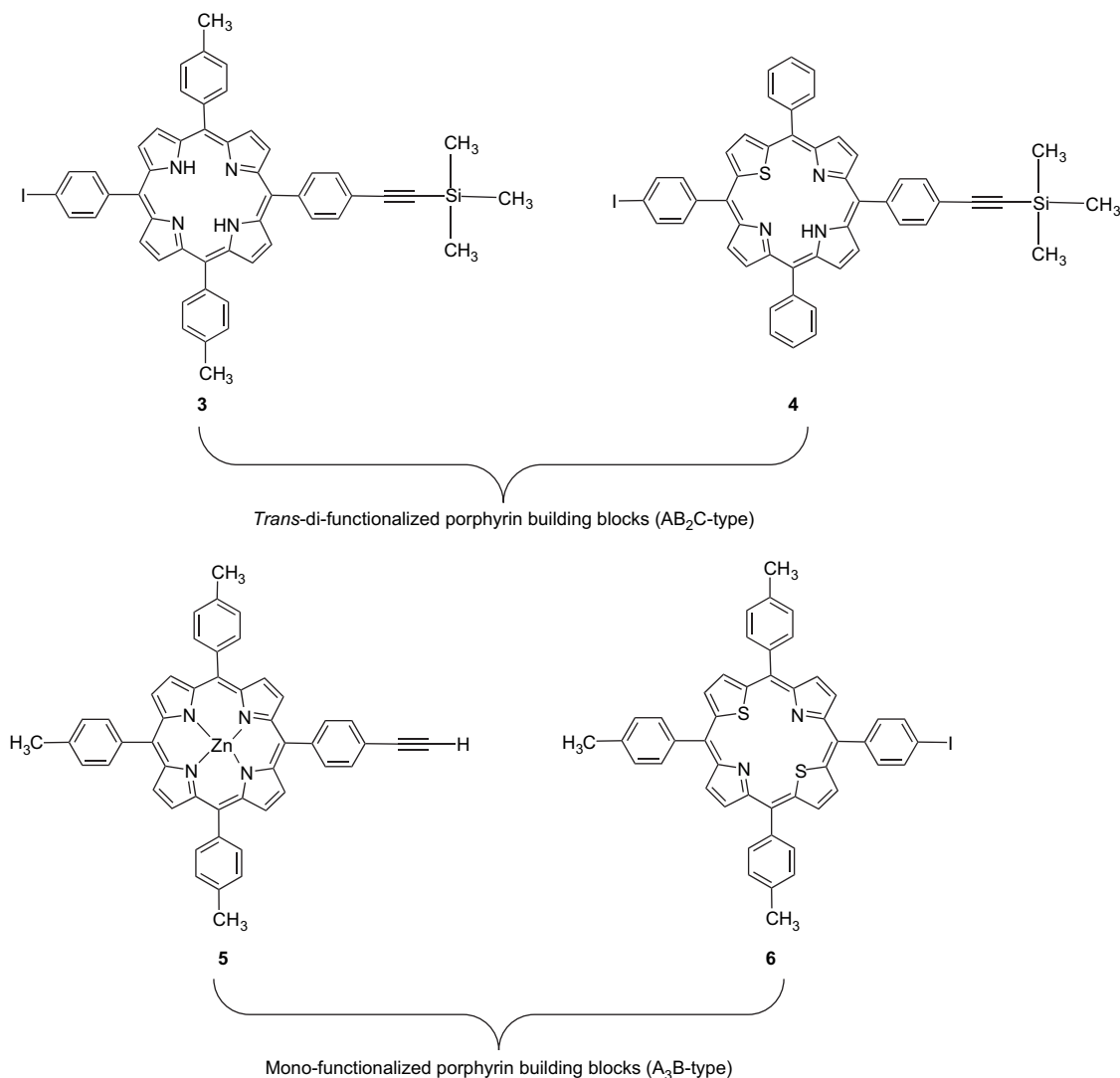


Chart 1. Linear porphyrin triad **1** and linear porphyrin tetrad **2**.



**Chart 2.** Trans di-functionalized and mono-functionalized porphyrin building blocks.

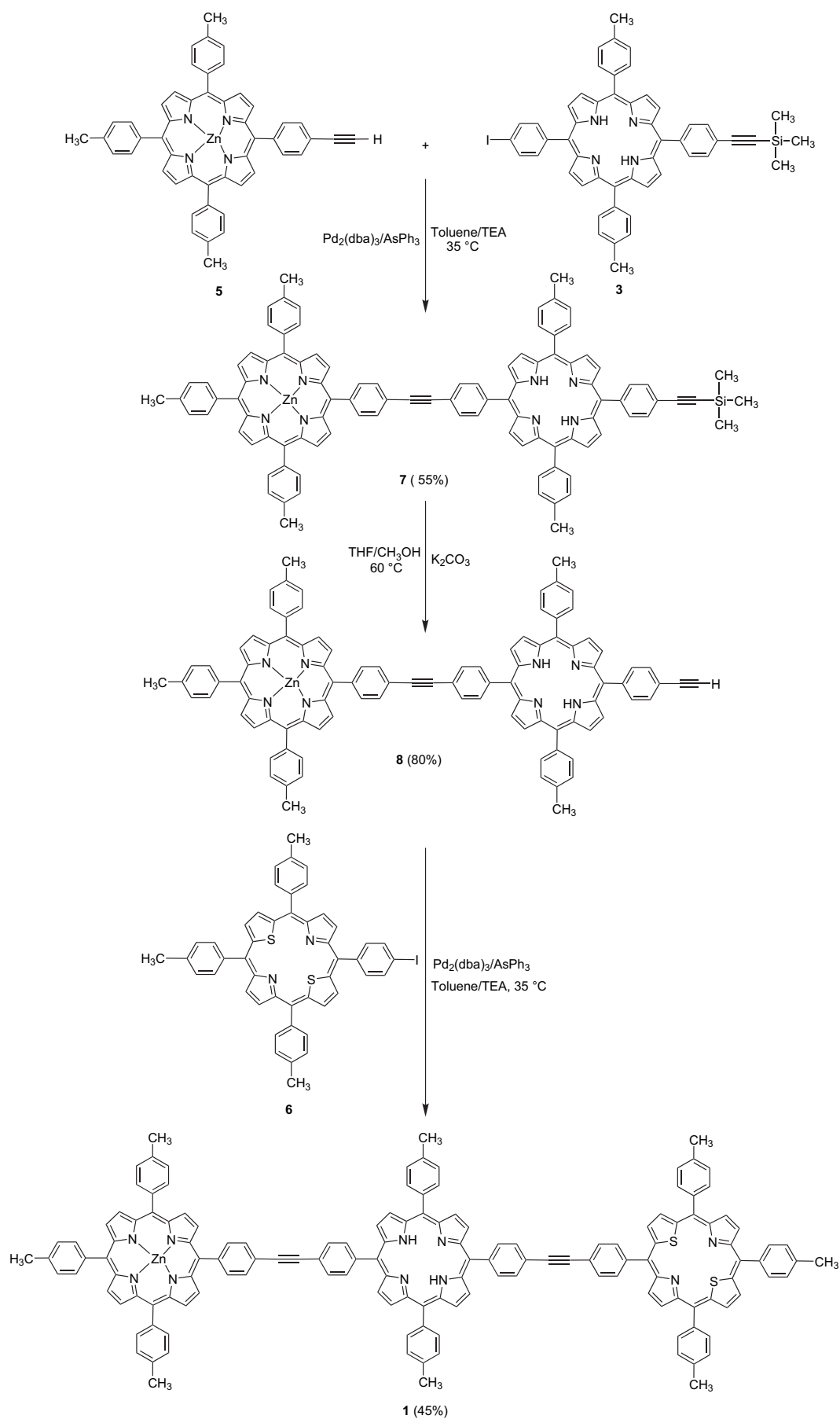
N<sub>3</sub>S porphyrin sub-units having one *meso*-phenylethynyl group on N<sub>3</sub>S porphyrin sub-unit, and (3) synthesis of linear tetrad having ZnN<sub>4</sub>, N<sub>4</sub>, N<sub>3</sub>S, and N<sub>2</sub>S<sub>2</sub> porphyrin sub-units. The ZnN<sub>4</sub>–N<sub>4</sub> porphyrin dyad having phenylethynyl group at the *meso*-position of N<sub>4</sub> porphyrin sub-unit **8** was synthesized as described above. The ZnN<sub>4</sub>–N<sub>4</sub>–N<sub>3</sub>S triad **9** was synthesized by coupling of dyad **8** and trans N<sub>3</sub>S porphyrin building block **4** in toluene/triethylamine at 35 °C in the presence of a catalytic amount of Pd<sub>2</sub>(dba)<sub>3</sub>/AsPh<sub>3</sub> (Scheme 2). The crude triad **9** was purified by column chromatography and characterized by spectroscopic techniques. The ES-MS and <sup>1</sup>H NMR spectra (Fig. 3a) confirmed the identity of the compound. In <sup>1</sup>H NMR spectrum of triad **9**, the 22 β-pyrrole protons, 8 belonging to ZnN<sub>4</sub> porphyrin sub-unit, 8 belonging to N<sub>4</sub> porphyrin sub-unit, and 6 belonging to N<sub>3</sub>S porphyrin sub-unit appeared as five sets of signals in δ 8.60–8.96 ppm region. The two β-thiophene protons appeared as two sets of well-defined doublets at δ 9.68 and 9.77 ppm. The inner NH protons appeared as two sets of broad singlets at δ –2.64 and –2.72 ppm corresponding to N<sub>3</sub>S and N<sub>4</sub> porphyrin sub-units, respectively. The triad **10** having *meso*-phenylethynyl group on N<sub>3</sub>S porphyrin sub-unit was obtained by treating triad **9** with K<sub>2</sub>CO<sub>3</sub> in THF/CH<sub>3</sub>OH at 60 °C followed by column chromatographic purification. The triad **10** was obtained by deprotection of ethynyl group of N<sub>3</sub>S porphyrin sub-unit of triad **9** and was confirmed by molecular ion peak in mass spectrum and a signal at δ 3.20 ppm corresponding

to ethynyl proton in <sup>1</sup>H NMR spectrum. The ZnN<sub>4</sub>–N<sub>4</sub>–N<sub>3</sub>S–N<sub>2</sub>S<sub>2</sub> tetrad **2** was prepared in the subsequent step by coupling of ZnN<sub>4</sub>–N<sub>4</sub>–N<sub>3</sub>S triad **10** and N<sub>2</sub>S<sub>2</sub> porphyrin building block **6** under identical palladium coupling conditions used for dyad **7** and triad **9**. The crude compound was subjected to column chromatographic purification and the pure tetrad **2** was obtained in 31% yield. The tetrad **2** was confirmed by molecular ion peak in ES-MS spectrum (Fig. 4) and clean <sup>1</sup>H NMR spectrum (Fig. 3b). In <sup>1</sup>H NMR spectrum of ZnN<sub>4</sub>–N<sub>4</sub>–N<sub>3</sub>S–N<sub>2</sub>S<sub>2</sub> tetrad **1**, the six β-thiophene protons, four corresponding to N<sub>2</sub>S<sub>2</sub> porphyrin sub-unit and two corresponding to N<sub>3</sub>S porphyrin sub-unit appeared as three resonances in δ 9.60–9.76 ppm region. The 26 β-pyrrole protons, 4 belonging to N<sub>2</sub>S<sub>2</sub> porphyrin sub-unit, 6 belonging to N<sub>3</sub>S porphyrin sub-unit, 8 belonging to N<sub>4</sub> porphyrin sub-unit, and 8 belonging to ZnN<sub>4</sub> porphyrin sub-unit appeared as seven sets of signals in δ 8.61–8.95 ppm region. The NH protons appeared as two sets of broad singlets at δ –2.65 and –2.82 ppm corresponding to N<sub>3</sub>S and N<sub>4</sub> porphyrin sub-units, respectively.

### 2.3. Absorption, electrochemical, and fluorescence properties of linear porphyrin triad **1** and tetrad **2**

#### 2.3.1. Absorption properties

The absorption spectra of porphyrin building blocks **3**, **4**, **5**, and **6**, dyad **7**, triads **1** and **9**, and tetrad **2** were recorded in toluene and

Scheme 1. Synthesis of linear porphyrin triad **1**.

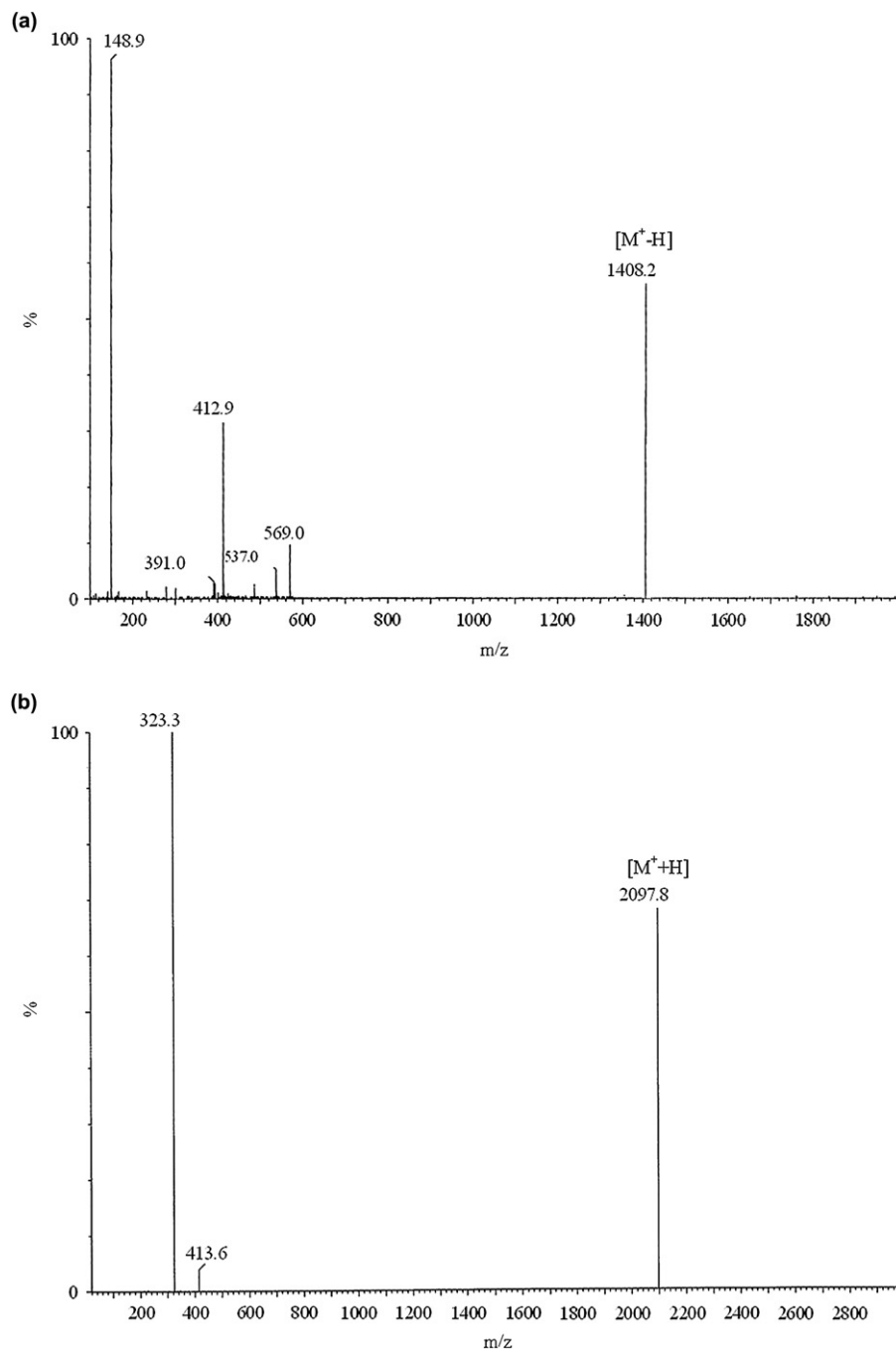


Figure 1. ES-MS spectrum of (a) porphyrin dyad **8** and (b) porphyrin triad **1**.

the data are tabulated in Table 1. A comparison of absorption spectra of dyad **7**, triad **9**, and tetrad **2** are shown in Figure 5. The dyad **7** containing  $ZnN_4$  and  $N_4$  porphyrin sub-units showed a broad Soret band at 423 nm (full width at half maxima=32 nm) and Q-bands at 515, 550, 590, and 648 nm. The triad **1** containing  $ZnN_4$ ,  $N_4$ , and  $N_2S_2$  porphyrin sub-units showed a broad Soret band with peak maxima at 429 nm and Q-bands at 516, 551, 590, 619, 640, and 697 nm. Thus, the absorption spectra of dyad **7** and triad **1** are essentially a linear combination of the spectra of the corresponding monomers with only minor differences in wavelength maxima and band shapes. Similarly, the triad **9** containing  $ZnN_4$ ,  $N_4$ , and  $N_3S$  porphyrin sub-units showed a broad split Soret band at 421 and 431 nm because of large differences in Soret absorption peak maxima of the corresponding porphyrin sub-units and six Q-bands at 516, 551, 590, 616, 648, and 678 nm. The tetrad **2**

containing  $ZnN_4$ ,  $N_4$ ,  $N_3S$ , and  $N_2S_2$  porphyrin sub-units also showed a broad splitted Soret band at 421 and 436 nm, and eight Q-bands at 514, 549, 590, 620, 633, 646, 678, and 696 nm. These observations indicate that the interaction between porphyrin sub-units in dyad, triads, and tetrad is weak and the porphyrin sub-units in these systems retain their individual identities. Similar observations were noted by Lindsey and co-workers in related systems.<sup>7–15</sup>

### 2.3.2. Electrochemical properties

The electrochemical properties of dyad **7**, triads **1** and **9**, tetrad **2**, and reference porphyrin monomers are probed through cyclic voltammetric and differential pulse voltammetric studies using tetrabutylammonium perchlorate (0.1 M) as supporting electrolyte in dichloromethane as solvent. The comparison cyclic voltammogram

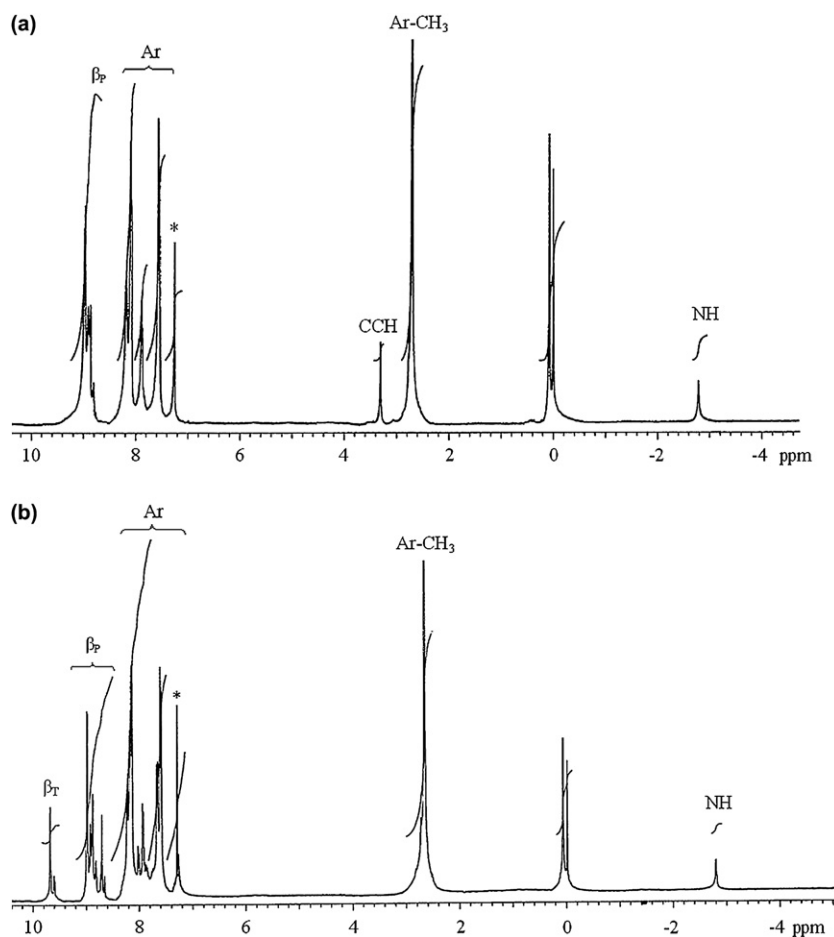


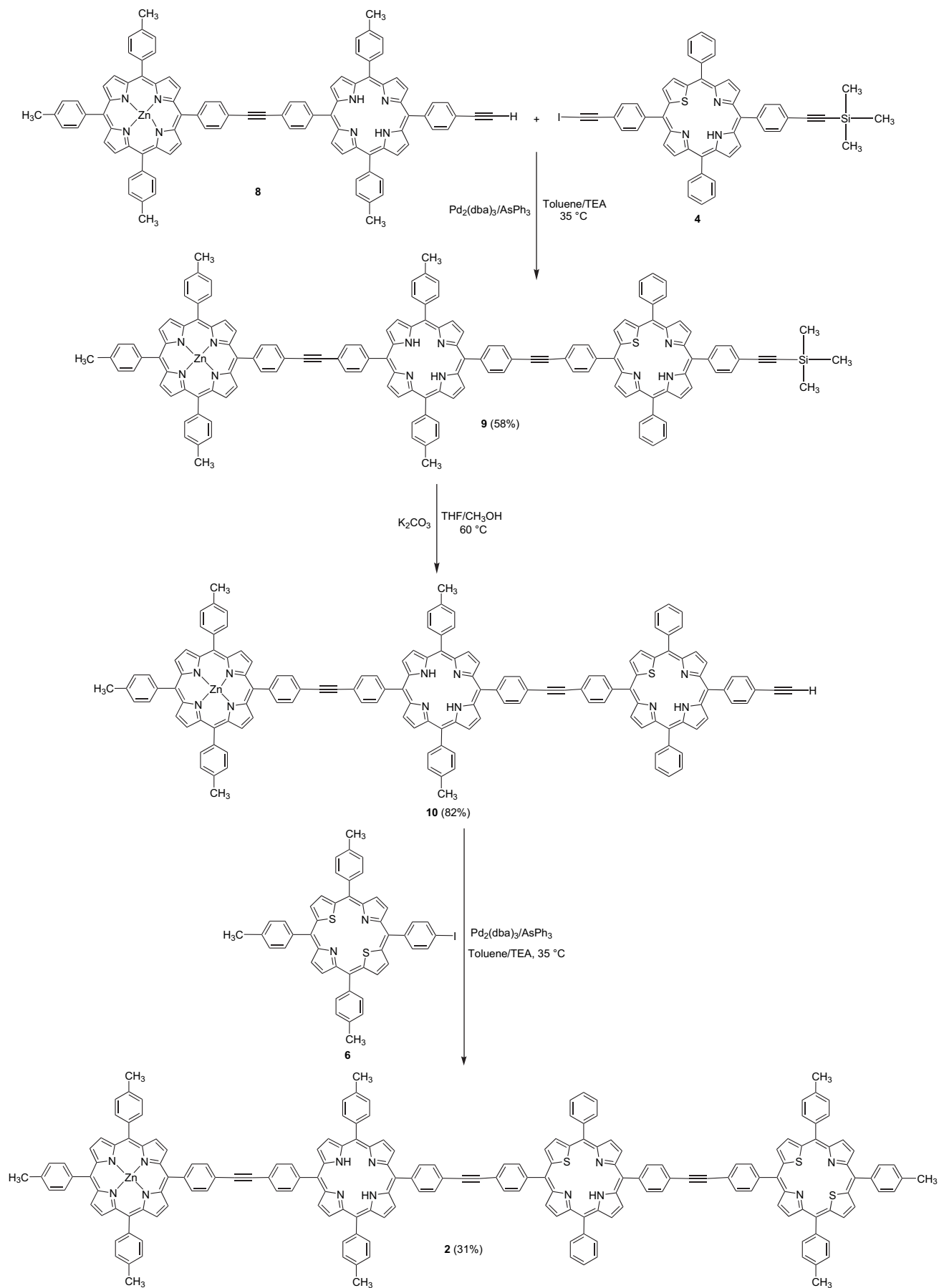
**Figure 2.** Comparison of  $^1\text{H}$  NMR spectra of (a) porphyrin dyad **8** and (b) porphyrin triad **1** recorded in  $\text{CDCl}_3$ . The peak with \* is due to solvent impurity.

oxidation waves of  $\text{ZnN}_4$  porphyrin **5**,  $\text{ZnN}_4\text{-N}_4$  porphyrin dyad **7**,  $\text{ZnN}_4\text{-N}_4\text{-N}_3\text{S}$  porphyrin triad **9**, and  $\text{ZnN}_4\text{-N}_4\text{-N}_3\text{S-N}_2\text{S}_2$  porphyrin tetrad **2** are shown in Figure 6a and the comparison of cyclic voltammogram reduction waves of triad **9** and tetrad **2** is shown in Figure 6b. All monomeric reference compounds exhibited two oxidation waves and two reduction waves corresponding to the formation of mono- and dications and mono- and dianions, respectively (Table 2).<sup>25,26</sup> The  $\text{ZnN}_4\text{-N}_4$  porphyrin dyad **7** showed three oxidations and four reductions and the potentials were in the same range of its corresponding monomers supporting a weak interaction between the porphyrin sub-units (Fig. 6a). The  $\text{ZnN}_4\text{-N}_4\text{-N}_2\text{S}_2$  porphyrin triad **1** showed two oxidations at 0.72 and 1.02 V and four reductions at -1.01, -1.20, -1.48, and -1.73 V. Comparison of redox potentials of triad **1** with its three porphyrin sub-units indicates that the triad **1** showed oxidation and reduction waves corresponding to all three porphyrin sub-units with no shifts supporting a weak interaction between the porphyrin sub-units. Similarly, the  $\text{ZnN}_4\text{-N}_4\text{-N}_3\text{S}$  porphyrin triad **9** also showed two oxidations and three reductions (Fig. 6). The porphyrin tetrad **2** showed three oxidation and four reduction waves corresponding to all four sub-units (Fig. 6). However, all oxidation and reduction waves were not resolved completely in tetrad **2** due to overlap of potentials of corresponding monomers. Thus, the electrochemical data are in line with the absorption data and supported a weak interaction between the porphyrin sub-units in triad **1** and tetrad **2**.

### 2.3.3. Fluorescence properties

The preliminary fluorescence properties of porphyrin dyad **7**, triads **1** and **9**, tetrad **2**, and the reference compounds were studied by steady state and time-resolved fluorescence techniques to

understand their excited state dynamics. The comparison of emission spectra of **5**,  $\text{ZnN}_4\text{-N}_4$  porphyrin dyad **7**, and  $\text{ZnN}_4\text{-N}_4\text{-N}_2\text{S}_2$  porphyrin triad **1** recorded at 550 nm is shown in Figure 7, and the comparison of emission spectra of  $\text{ZnN}_4\text{-N}_4\text{-N}_3\text{S}$  triad **9** and  $\text{ZnN}_4\text{-N}_4\text{-N}_3\text{S-N}_2\text{S}_2$  porphyrin tetrad **2** are shown in Figure 8. The photophysical data of porphyrin triads **1** and **9**, tetrad **2**, and other relevant compounds are presented in Table 3. Consistent with the studies reported in the literature on similar type of  $\text{ZnN}_4\text{-N}_4$  porphyrin dyads,<sup>7-10</sup> the  $\text{ZnN}_4\text{-N}_4$  porphyrin dyad **7** exhibited an efficient singlet energy transfer from the  $\text{ZnN}_4$  porphyrin sub-unit to the  $\text{N}_4$  porphyrin sub-unit on excitation at  $\text{ZnN}_4$  porphyrin sub-unit. Thus dyad **7** on excitation at 550 nm, where  $\text{ZnN}_4$  porphyrin sub-unit absorbs strongly, the emission from the  $\text{ZnN}_4$  component of dyad **7** is significantly quenched (98%,  $\phi=0.00066$ ), while that of the  $\text{N}_4$  component is enhanced (Fig. 7b). These observations support the energy transfer from  $\text{ZnN}_4$  porphyrin sub-unit to  $\text{N}_4$  porphyrin sub-unit in porphyrin dyad **7**. Similarly, in the triad **1**, excitation at 550 nm where  $\text{ZnN}_4$  porphyrin sub-unit absorbs strongly, we expected a major emission from  $\text{N}_2\text{S}_2$  porphyrin sub-unit if energy transfer occurs efficiently from  $\text{ZnN}_4$  porphyrin sub-unit to  $\text{N}_2\text{S}_2$  porphyrin sub-unit mediated by  $\text{N}_4$  porphyrin sub-unit. The emission spectrum showed in Figure 7c indicates that the  $\text{ZnN}_4$  porphyrin emission was quenched by 98% and the  $\text{N}_4$  emission was quenched by 87% and the major emission was noted from  $\text{N}_2\text{S}_2$  porphyrin sub-unit. The excitation spectrum of triad **1** recorded at emission wavelength 720 nm matches very closely with the absorption spectrum. Although major emission was observed from  $\text{N}_2\text{S}_2$  porphyrin sub-unit in triad **1** on excitation at  $\text{ZnN}_4$  porphyrin sub-unit, the 13% emission, which was leaked from  $\text{N}_4$  porphyrin sub-unit indicate that the energy transfer from  $\text{ZnN}_4$

Scheme 2. Synthesis of linear porphyrin tetrad **2**.



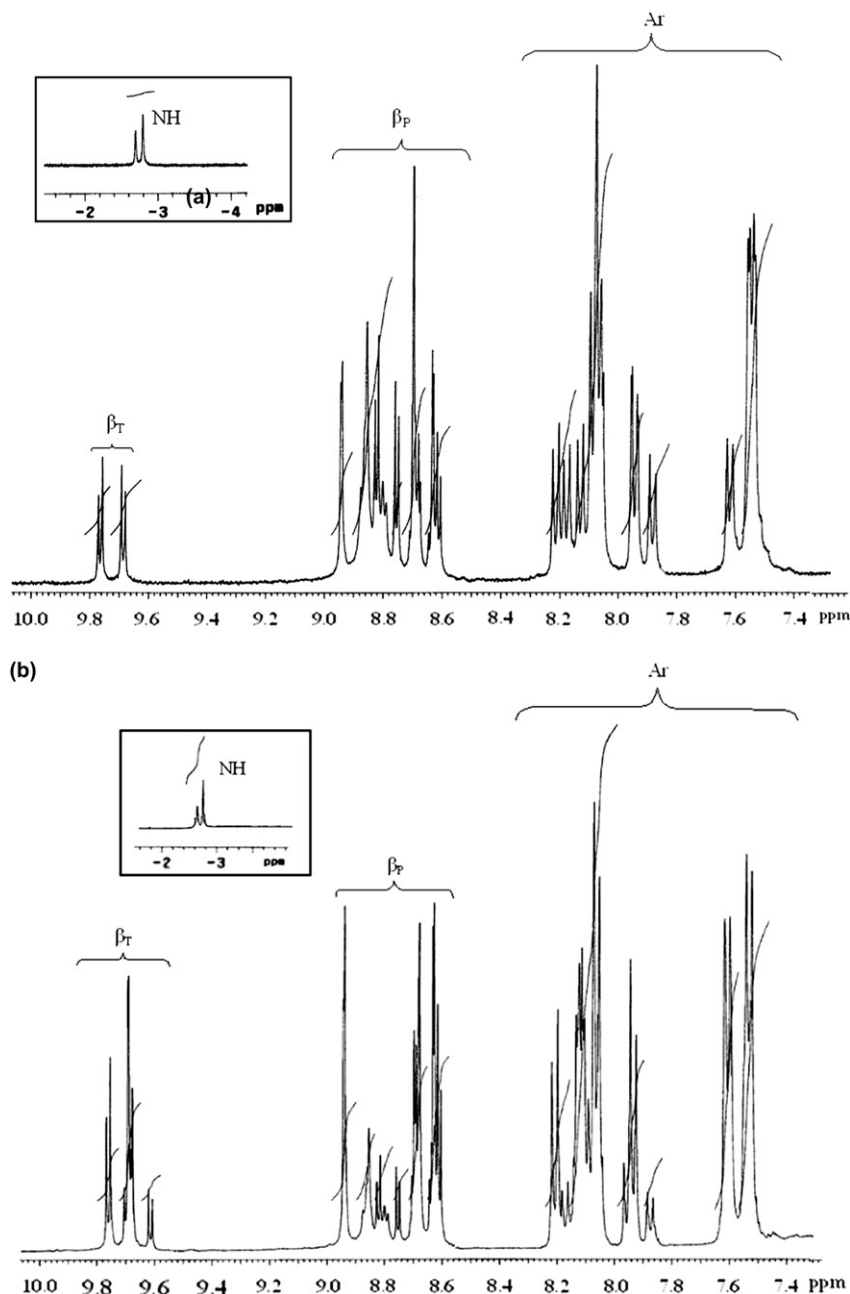


**Figure 3.** Comparison of  $^1\text{H}$  NMR spectra of selected protons of (a) porphyrin triad **9** and (b) porphyrin tetrad **2** recorded in  $\text{CDCl}_3$ . The NH signals are shown in insets.

porphyrin sub-unit to  $\text{N}_2\text{S}_2$  porphyrin sub-unit mediated via  $\text{N}_4$  porphyrin sub-unit is not very efficient. The steady state fluorescence studies were carried for tetrad **2** and triad **9** by exciting at 550 nm where  $\text{ZnN}_4$  porphyrin sub-unit absorbs strongly. The comparison of emission spectra of triad **9** and tetrad **2** recorded at 550 nm is shown in Figure 8. As evident in Figure 8a,  $\text{ZnN}_4$ – $\text{N}_4$ – $\text{N}_3\text{S}$  triad **9**, on excitation at 550 nm, where  $\text{ZnN}_4$  porphyrin sub-unit absorbs strongly, the emission was noted from both  $\text{N}_4$  and  $\text{N}_3\text{S}$  porphyrin sub-units indicating that the energy transfer from  $\text{ZnN}_4$  porphyrin sub-unit to  $\text{N}_3\text{S}$  porphyrin sub-unit mediated by  $\text{N}_4$  porphyrin sub-unit is not very efficient. This is similar to what we observed for triad **1** in which the energy transfer from  $\text{ZnN}_4$  porphyrin sub-unit to  $\text{N}_2\text{S}_2$  porphyrin sub-unit mediated by  $\text{N}_4$  was not very efficient. However, when  $\text{ZnN}_4$ – $\text{N}_4$ – $\text{N}_3\text{S}$ – $\text{N}_2\text{S}_2$  porphyrin tetrad **2** was recorded at 550 nm, the emission from  $\text{ZnN}_4$ ,  $\text{N}_4$ , and  $\text{N}_3\text{S}$  porphyrin sub-units was quenched significantly and the major emission was noted from terminal  $\text{N}_2\text{S}_2$  porphyrin sub-unit. The

excitation spectrum of tetrad **2** recorded at 720 nm matches with its absorption spectrum. These results support an efficient energy transfer in tetrad **2** from  $\text{ZnN}_4$  porphyrin sub-unit to  $\text{N}_2\text{S}_2$  porphyrin sub-unit mediated by  $\text{N}_4$  and  $\text{N}_3\text{S}$  porphyrin sub-units. Thus, if four porphyrin sub-units having energy levels in cascade manner are arranged linearly, the energy transfer from one end to other end is very efficient.

The preliminary time-resolved studies were carried out on dyad **7**, triads **1** and **9**, tetrad **2**, and reference porphyrin monomers by exciting at 406 nm in toluene at room temperature. The observed lifetimes of reference porphyrin monomers measured at their corresponding emission peak maxima were identical with the reported literature values (Table 3). A representative fluorescence decay curve for porphyrin tetrad **2** is shown in Figure 9. The fluorescence lifetime of dyad **7** was measured by monitoring the decay at 600 and 650 nm corresponding to the  $\text{ZnN}_4$  and  $\text{N}_4$  porphyrin sub-units of dyad. When the emission decay of dyad was measured



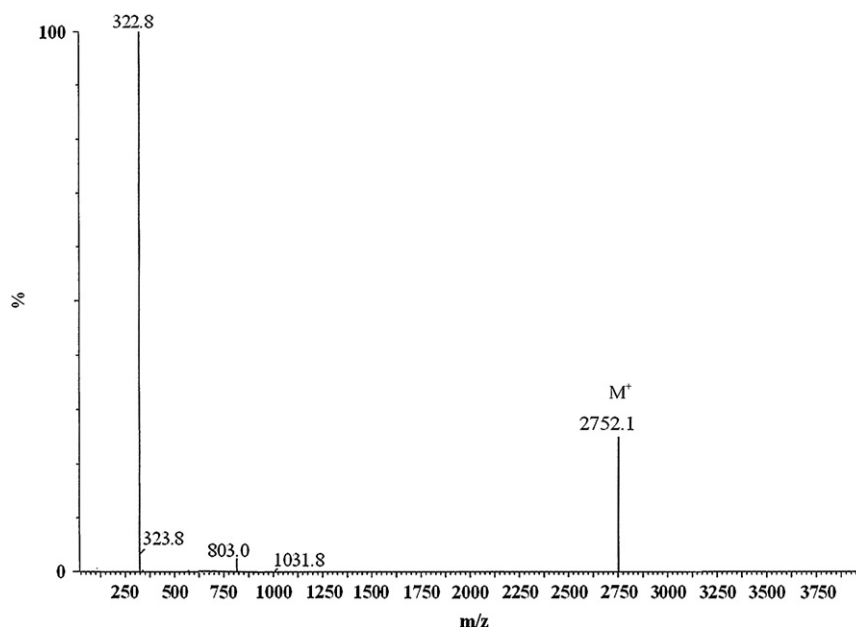


Figure 4. ES-MS spectrum of linear porphyrin tetrad 2.

Table 1

Absorption data of dyad **7**, triads **1** and **9**, and tetrad **2** and their corresponding monomers recorded in toluene

Porphyrin	Soret band $\lambda$ (nm) ( $\epsilon \times 10^{-4}$ , $\text{dm}^3 \text{mol}^{-1} \text{cm}^{-1}$ )	Absorption Q-bands $\lambda$ (nm) ( $\epsilon \times 10^{-3}$ , $\text{dm}^3 \text{mol}^{-1} \text{cm}^{-1}$ )
<b>3</b>	420 (45.2)	516 (22.2), 551 (9.5), 593 (6.4), 649 (5.5)
<b>4</b>	430 (18.6)	514 (15.5), 549 (5.4), 617 (2.4), 678 (3.8)
<b>5</b>	423 (40.6)	550 (16.6), 588 (1.9)
<b>6</b>	437 (21.3)	514 (19.3), 548 (5.8), 633 (1.4), 697 (3.5)
<b>7</b>	423 (30.5)	515 (20.5), 550 (14.4), 590 (5.5), 648 (4.0)
<b>1</b>	429 (38.4)	516 (33.2), 551 (15.0), 590 (2.2), 619 (2.9), 640 (sh), 697 (3.5)
<b>9</b>	421 (sh), 431 (20.8)	516 (20.2), 551 (32.2), 590 (2.2), 616 (2.8), 648 (2.9), 678 (1.5)
<b>2</b>	421 (sh), 436 (43.8)	514 (42.5), 549 (11.0), 590 (2.4), 620 (1.2), 633 (1.4), 646 (2.0), 678 (2.4), 696 (1.2)

at 650 nm, the decay is monophasic with  $\tau_f$  of 9.2 ns as expected. However, when decay of dyad **7** was monitored at 600 nm, the fluorescence decay curve is biphasic. The shorter lifetime component (65 ps) accounts for the major emission of decay (98%) along

with minor long component decay at 2.1 ns (2%). The minor long component decay at 2.1 ns is due to  $\text{ZnN}_4$  porphyrin impurity present in the dyad **7** and the major component decay at 65 ps is due to the decreased lifetime of the  $\text{ZnN}_4$  porphyrin sub-unit because of the transfer of energy from  $\text{ZnN}_4$  porphyrin sub-unit to  $\text{N}_4$  porphyrin sub-unit. These observations were line with the literature reports on similar type of porphyrin dyads.<sup>7–10</sup> The  $\text{ZnN}_4$ – $\text{N}_4$ – $\text{N}_2\text{S}_2$  porphyrin triad **1** emission decay monitored at 600 nm was triphasic with one major component (187 ps, 97%) and two minor components (2.6 and 8.57 ns, 3%). The major component at 187 ps is the decreased lifetime of  $\text{ZnN}_4$  porphyrin sub-unit because of the transfer of its energy to  $\text{N}_2\text{S}_2$  porphyrin sub-unit mediated by  $\text{N}_4$  porphyrin sub-unit. When the decay of tetrad **2** is monitored at 600 nm, the fluorescence decay curve is biphasic (Fig. 9). The shorter lifetime component (117 ps) accounts for the major emission of decay (97%) along with the minor longer component decay at 9.1 ns. The minor lifetime component at 9.1 ns is attributed to the  $\text{N}_4$  porphyrin impurity present in the tetrad **2**, and the major component at 117 ps is the decreased lifetime of  $\text{ZnN}_4$  porphyrin sub-unit because of the transfer of its energy to  $\text{N}_2\text{S}_2$  porphyrin sub-unit via  $\text{N}_4$  and  $\text{N}_3\text{S}$  porphyrin sub-units. From the measured lifetime of the  $\text{ZnN}_4$  porphyrin sub-unit in dyad **7**, triad **9**, and tetrad **2** ( $\tau_{\text{donor-acceptor}}$ ) and the lifetime of  $\text{ZnTPP}$  ( $\tau_{\text{donor}}$ ), the rate constant of energy transfer ( $K_{\text{ENT}}^{-1}$ ) and the yield of energy transfer ( $\phi_{\text{ENT}}$ ) from the  $\text{ZnN}_4$  porphyrin sub-unit to terminal  $\text{N}_2\text{S}_2$  porphyrin sub-unit in triad **1** and tetrad **2** were calculated using Eqs. 1 and 2.<sup>7</sup>

$$K_{\text{ENT}} = 1/\tau_{\text{donor-acceptor}} - 1/\tau_{\text{donor}} \quad (1)$$

$$\phi_{\text{ENT}} = K_{\text{ENT}}\tau_{\text{donor-acceptor}} \quad (2)$$

The data presented in Table 3 indicate that for tetrad **2**, the rate of excitation energy transfer ( $K_{\text{ENT}}^{-1}$ ) is 124 ps and the yield of energy transfer ( $\phi_{\text{ENT}}$ ) is 94%. The rate of energy transfer for tetrad **2** is slower as compared to diarylethynyl bridged porphyrin arrays containing  $\text{N}_4$  porphyrin sub-units, which is tentatively attributed to the presence of three sulfur atoms in two porphyrin sub-units of tetrad **2**, which enhances the contribution of non-radiative decay channels.

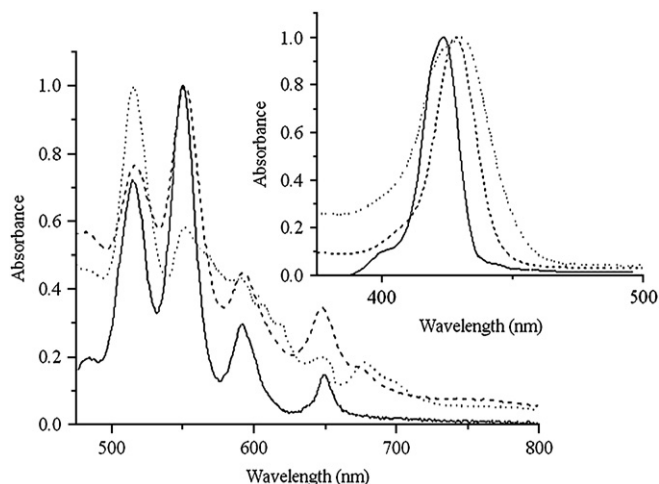
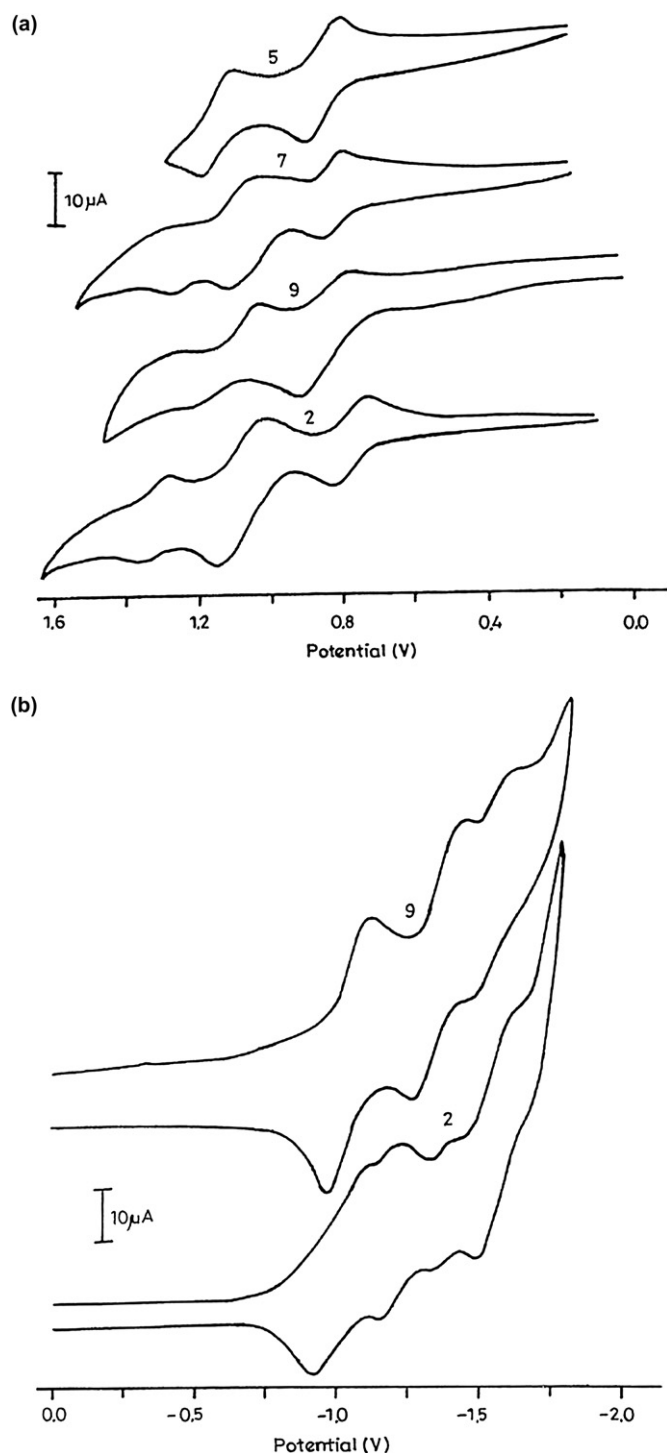


Figure 5. Q-band absorption spectra of **7** (—), **9** (---) and **2** (···) recorded in toluene. Their corresponding Soret band absorption spectra are shown in inset. The concentration used for Q-band spectra was  $5 \times 10^{-5}$  M and for Soret band was  $5 \times 10^{-6}$  M.



**Figure 6.** Comparison of (a) cyclic voltammogram oxidation waves of **5**, **7**, **9**, and **2**, and (b) cyclic voltammogram reduction waves of **9** and **2** in  $\text{CH}_2\text{Cl}_2$  containing TBAP (0.1 M) recorded at  $50 \text{ mV s}^{-1}$  versus SCE. The concentrations used were  $\sim 10^{-3} \text{ M}$ .

### 3. Conclusion

In summary, we synthesized a linear diarylethyne bridged porphyrin triad containing  $\text{ZnN}_4$ ,  $\text{N}_4$ , and  $\text{N}_2\text{S}_2$  porphyrin sub-units and linear porphyrin tetrad containing  $\text{ZnN}_4$ ,  $\text{N}_4$ ,  $\text{N}_3\text{S}$ , and  $\text{N}_2\text{S}_2$  porphyrin sub-units under  $\text{Pd(0)}$  mediated coupling conditions over sequence of steps. The coupling reactions worked smoothly and the compounds were obtained in decent yields. The porphyrin triad and tetrad are freely soluble in common organic solvents and were characterized by various spectroscopic techniques. The NMR,

**Table 2**

Electrochemical redox data (V) of compounds dyad **7**, triads **1** and **9**, and tetrad **2** and their reference porphyrin monomers recorded in dichloromethane containing 0.1 M tetrabutylammonium perchlorate as supporting electrolyte

Compound	Oxidation				Reduction					
	I	II	III	IV	I	II	III	IV	V	VI
<b>3</b>	—	0.96	—	1.32	—	—	−1.19	—	−1.53	—
<b>4</b>	—	1.04	—	—	−1.06	−1.27	—	—	—	—
<b>5</b>	0.77	—	1.11	—	—	—	—	−1.35	—	−1.73
<b>6</b>	—	—	1.18	—	−0.95	—	−1.17	—	—	—
<b>7</b>	0.74	1.02	—	1.30	—	—	−1.18	−1.34	−1.55	−1.74
<b>1</b>	0.72	1.02	—	—	—	−1.01	−1.20	—	−1.48	−1.73
<b>9</b>	0.72	0.99	—	—	—	−1.11	—	—	−1.44	−1.60
<b>2</b>	0.72	0.97	1.02	1.28	−0.96	−1.10	−1.24	—	−1.41	−1.60

absorption, and electrochemical studies indicated that the porphyrin sub-units in triad and tetrad interact very weakly and the porphyrin sub-units retain their identities in these systems. The steady state and time-resolved fluorescence studies supported an energy transfer from one end of the porphyrin array to the other end. More photophysical studies are required to quantify these observations. These kinds of porphyrin triads and tetrads containing different porphyrin sub-units will have potential application in opto-electronic devices and other materials.

## 4. Experimental

### 4.1. General

5-(4-Iodophenyl)-15-{4-[2-(trimethylsilyl)ethynyl]phenyl}-10,20-di(*p*-tolyl)porphyrin (**3**),<sup>22</sup> 5-(4-iodophenyl)-15-{4-[2-(trimethylsilyl)ethynyl]phenyl}-10,20-diphenyl-21-thiaporphyrin (**4**),<sup>21</sup> 5-(4-ethynylphenyl)-10,15,20-tri(*p*-tolyl)zinc(II)porphyrin (**5**),<sup>23</sup> and 5-(4-iodophenyl)-10,15,20-tri(*p*-tolyl)-21,23-dithiaporphyrin (**6**)<sup>17</sup> were prepared by following the literature methods.  $^1\text{H}$  and  $^{13}\text{C}$  NMR spectra were recorded on a Varian 400 MHz spectrometer using tetramethylsilane (TMS) as an internal standard and are reported in  $\delta$  (ppm), referred to  $^1\text{H}$  (of residual proton;  $\delta$  7.26) and  $^{13}\text{C}$  ( $\delta$  77.0) signals of  $\text{CDCl}_3$ . Absorption spectra were obtained with SHIMADZU UV-160 spectrometer. Infrared spectra were recorded on a Nicolet Impact-400 FT-IR spectrometer and the ES-MS spectra were recorded with a Q-ToF micro (YA-105) mass spectrometer. Fluorescence spectra were recorded at  $25^\circ\text{C}$  in a 1 cm quartz fluorescence cuvette on a Perkin-Elmer LS 55 luminescence spectrometer. Cyclic voltammetric (CV) and differential pulse voltammetric (DPV) studies were carried out with BAS electrochemical system utilizing the three electrode configuration consisting of a glassy carbon (working electrode), platinum wire (auxiliary electrode), and saturated calomel (reference electrode) electrodes. The experiments were done in dry dichloromethane using 0.1 M tetrabutylammonium perchlorate as supporting electrolyte. Half wave potentials were measured using DPV and also calculated manually by taking the average of the cathodic and anodic peak potentials. The solvents such as THF and toluene were obtained from S.D. Fine chemicals, India, and dried over sodium benzophenone ketyl and distilled prior to use. Triethylamine was dried over  $\text{CaH}_2$  and distilled prior to use. Trimethylsilylacetylene, tris(dibenzylideneacetone)dipalladium(0), and triphenylarsine were used as obtained from Sigma-Aldrich Chemical Co. All other chemicals used for the synthesis were of reagent grade unless otherwise specified. Column chromatography was performed on silica (Merck, 60–120 mesh) obtained from Sisco Research Laboratories, India.

#### 4.1.1. $\text{ZnN}_4$ - $\text{N}_4$ porphyrin dyad **7**

A solution of  $\text{ZnN}_4$  porphyrin **5** (50 mg, 0.07 mmol) and 5-[4-(2-trimethylsilyl)phenyl]-10-(4-iodophenyl)-15,20-di(*p*-tolyl)porphyrin

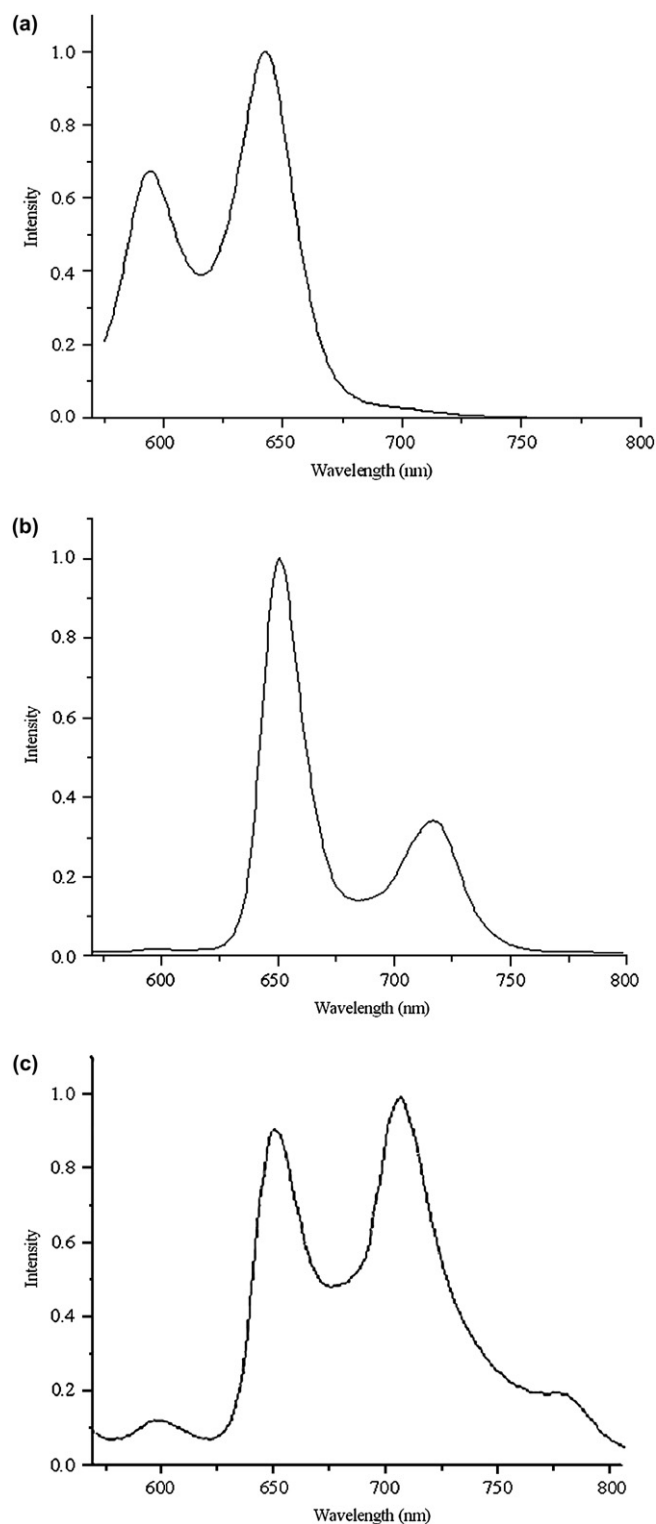


**Figure 7.** Comparison of emission spectra of (a) **5**, (b) **7**, and (c) **1** recorded in toluene at  $\lambda_{\text{ex}}=600$  nm.

**3** (45 mg, 0.07 mmol) in dry toluene/triethylamine (3:1, 30 mL) was purged with nitrogen for 15 min. The coupling was initiated by adding  $\text{AsPh}_3$  (15 mg, 0.06 mmol) followed by  $\text{Pd}_2(\text{dba})_3$  (6 mg, 0.03 mmol) and the reaction mixture was then stirred at 35 °C for 12 h. TLC analysis indicated the appearance of new spot apart from the corresponding monomeric spots. The crude reaction mixture was purified by silica gel chromatography using petroleum ether/dichloromethane as eluent. The excess  $\text{AsPh}_3$  and small amounts of unreacted

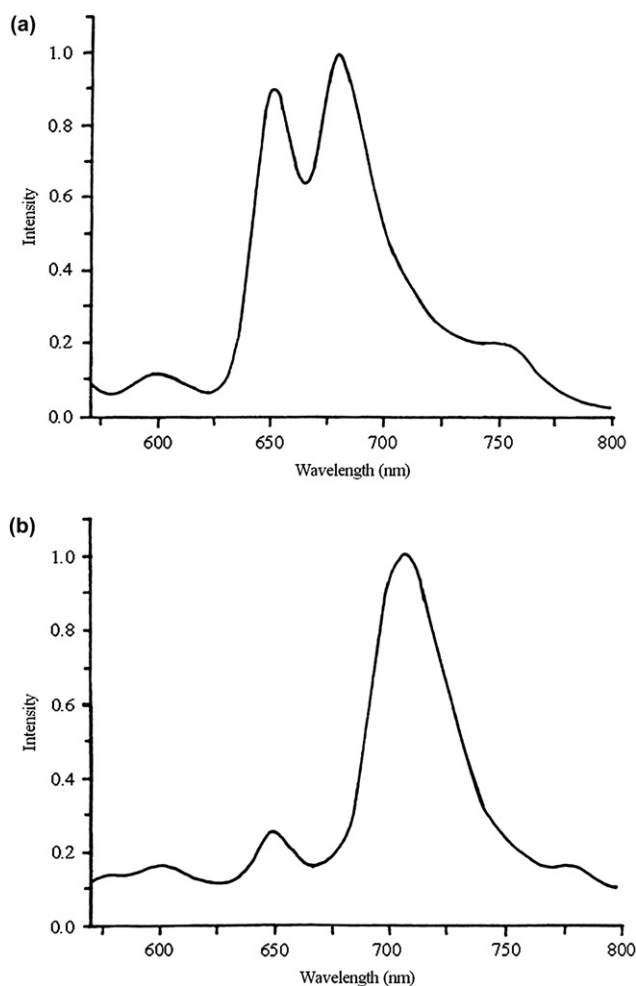


**Figure 8.** Comparison of emission spectra of (a) **9** and (b) **2** recorded in toluene at  $\lambda_{\text{ex}}=600$  nm.

monomers were removed using petroleum ether/dichloromethane (80:20) and the dyad **7** was then collected using petroleum ether/dichloromethane (60:40) in 55% yield (57 mg). Mp >300 °C. IR (KBr film):  $\nu=3073, 2940, 2862, 1452, 990, 750 \text{ cm}^{-1}$ .  $^1\text{H}$  NMR (400 MHz,  $\text{CDCl}_3$ , 25 °C):  $\delta=-2.78$  (br s, 2H, NH), 0.38 (s, 9H, Si- $\text{CH}_3$ ), 2.74 (s, 15H, Ar- $\text{CH}_3$ ), 7.56 (d,  $J=8.2$  Hz, 10H, Ar), 7.88 (d,  $J=8.0$  Hz, 6H, Ar), 8.00 (d,  $J=8.2$  Hz, 10H, Ar), 8.18 (d,  $J=7.6$  Hz, 6H, Ar), 8.78–9.00 (m, 16H,

**Table 3**

Photophysical data of porphyrin dyad **7**, triads **1** and **9**, and tetrad **2** and their corresponding reference porphyrin monomers recorded in toluene

Compound	$\Phi_f$ (donor)	% donor <sup>a</sup>	$\tau_{\text{DA}}^b$ (ps)	$\Phi_{\text{ENT}}$	$K_{\text{ENT}}^{-1}$ (ps)
<b>3</b>	0.11	—	9240	—	—
<b>4</b>	0.016	—	1334	—	—
<b>5</b>	0.0331	—	2070	—	—
<b>6</b>	0.007	—	1224	—	—
<b>7</b>	0.0006	98	65	0.98	67
<b>1</b>	0.0042	87	187	0.91	206
<b>9</b>	0.0029	91	135	0.93	144
<b>2</b>	0.0011	97	117	0.94	124

<sup>a</sup> Calculated using the equation

$$\% \text{ of donor emission quenched} = \left(1 - \frac{\Phi_{\text{DA}}}{\Phi_{\text{D}}}\right) \times 100$$

$\Phi_{\text{DA}}$ =quantum yield of donor porphyrin sub-unit in dyad DA.

$\Phi_{\text{D}}$ =quantum yield of donor porphyrin.

<sup>b</sup> The experimentally observed lifetime of donor porphyrin monomer and donor porphyrin sub-unit in dyad, triad, and tetrad.

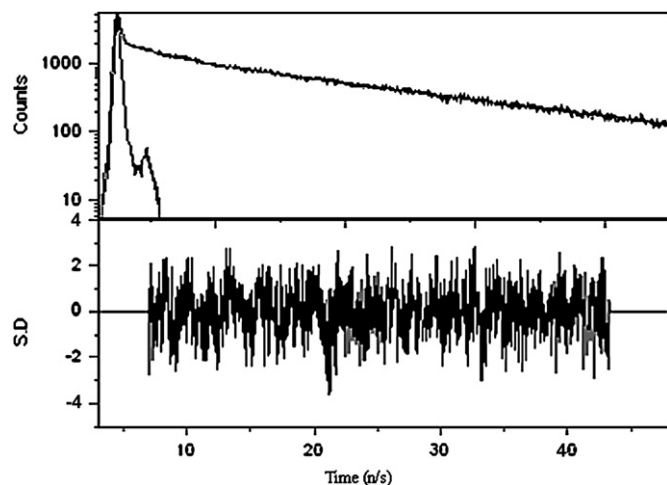


**Figure 9.** Fluorescence decay profile and weighed residuals fit of tetrad **2**. The excitation wavelength used was 406 nm and emission was detected at 600 nm.

$\beta$ -pyrrole) ppm.  $^{13}\text{C}$  NMR (100 MHz,  $\text{CDCl}_3$ , 25 °C):  $\delta$ =22.7, 25.7, 90.5, 100.0, 124.4, 126.7, 127.2, 127.8, 128.2, 13.5, 131.2, 131.7, 132.8, 133.1, 134.3, 134.8, 138.3, 143.3, 146.9, 147.5 ppm. ES-MS:  $\text{C}_{100}\text{H}_{74}\text{N}_8\text{SiZn}$ , calcd av mass 1481.2, obsd  $m/z$  1480.3 [ $\text{M}^+ - \text{H}$ , 70%].

#### 4.1.2. $\text{ZnN}_4\text{-N}_4$ porphyrin dyad **8**

The desired dyad **8** having a phenylethynyl group was obtained by treating 1 equiv of porphyrin dyad **7** (20 mg, 0.013 mmol) with 10 equiv of  $\text{K}_2\text{CO}_3$  (18.6 mg, 0.13 mmol) in THF/ $\text{CH}_3\text{OH}$  under refluxing condition. The solvent was removed on rotary evaporator under vacuum and obtained dyad **8** as a purple solid (15 mg, 80%). Mp >300 °C. IR (KBr film):  $\nu$ =3326, 3073, 2940, 2862, 1452, 990, 750  $\text{cm}^{-1}$ .  $^1\text{H}$  NMR (400 MHz,  $\text{CDCl}_3$ , 25 °C):  $\delta$ =−2.78 (br s, 2H, NH), 3.33 (s, 1H, CH), 2.74 (s, 15H, Ar-CH<sub>3</sub>), 7.56 (d,  $J$ =8.2 Hz, 10H, Ar), 7.88 (d,  $J$ =8.0 Hz, 6H, Ar), 8.00 (d,  $J$ =8.2 Hz, 10H, Ar), 8.18 (d,  $J$ =7.6 Hz, 6H, Ar), 8.78–9.00 (m, 16H,  $\beta$ -pyrrole) ppm.  $^{13}\text{C}$  NMR (100 MHz,  $\text{CDCl}_3$ , 25 °C):  $\delta$ =22.7, 25.7, 90.5, 100.0, 124.4, 126.7, 127.2, 127.8, 128.2, 13.5, 131.2, 131.7, 132.8, 133.1, 134.3, 134.8, 138.3, 143.3, 146.9, 147.5 ppm. ES-MS:  $\text{C}_{97}\text{H}_{66}\text{N}_8\text{Zn}$ , calcd av mass 1409.1, obsd  $m/z$  1408.3 [ $\text{M}^+ - \text{H}$ , 54%].

#### 4.1.3. $\text{ZnN}_4\text{-N}_4\text{-N}_2\text{S}_2$ porphyrin triad (**1**)

A solution of  $\text{ZnN}_4\text{-N}_4$  dyad **8** (35 mg, 0.025 mmol) and 5-(4-iodophenyl)-10,15,20-tri(*p*-tolyl)-21,23-dithiaporphyrin **6** (20 mg, 0.025 mmol) in dry toluene/triethylamine (3:1, 30 mL) was purged with nitrogen for 10 min. The coupling was initiated by adding  $\text{AsPh}_3$  (9.2 mg, 0.032 mmol) followed by  $\text{Pd}_2(\text{dba})_3$  (4.5 mg, 0.008 mmol) and the reaction mixture was then stirred at 40 °C for 12 h. The excess  $\text{AsPh}_3$  and the minor amounts of starting porphyrins were removed on silica gel column using petroleum ether/dichloromethane (50:50) and the pure desired porphyrin triad **1** was collected with petroleum ether/dichloromethane (20:80) in 45% yield (19 mg). Mp >300 °C. IR (KBr film):  $\nu$ =3070, 2944, 2863, 1455, 990, 842, 745  $\text{cm}^{-1}$ .  $^1\text{H}$  NMR (400 MHz,  $\text{CDCl}_3$ , 25 °C):  $\delta$ =−2.76 (br s, 2H, NH), 2.78 (s, 24H, Ar-CH<sub>3</sub>), 7.52 (d,  $J$ =8.0 Hz, 8H, Ar), 7.62 (d,  $J$ =8.0 Hz, 12H, Ar), 7.76 (d,  $J$ =8.0 Hz, 8H, Ar), 7.98 (d,  $J$ =7.6 Hz, 4H, Ar), 8.08–8.20 (m, 16H, Ar), 8.62–8.70 (m, 4H,  $\beta$ -pyrrole), 8.76–8.82 (m, 8H,  $\beta$ -pyrrole), 8.90–8.98 (m, 8H,  $\beta$ -pyrrole), 9.62 (d,  $J$ =4.0 Hz, 1H,  $\beta$ -thiophene), 9.68–9.72 (m, 3H,  $\beta$ -thiophene) ppm.  $^{13}\text{C}$  NMR (100 MHz,  $\text{CDCl}_3$ , 25 °C):  $\delta$ =25.7, 89.7, 90.5, 124.4, 126.7, 127.2, 127.8, 128.2, 129.5, 131.7, 132.8, 133.2, 134.3, 134.8, 135.3, 138.3, 146.9, 147.5, 149.3, 150.2, 151.7, 153.4 ppm. ES-MS:  $\text{C}_{144}\text{H}_{98}\text{N}_{10}\text{S}_2\text{Zn}$ , calcd av mass 2096.8, obsd  $m/z$  2097.8 [ $\text{M}^+ - \text{H}$ , 63%].

#### 4.1.4. $\text{ZnN}_4\text{-N}_4\text{-N}_3\text{S}$ porphyrin triad (**9**)

A solution of dyad **8** (30 mg, 0.007 mmol) and **4** (6 mg, 0.007 mmol) in dry toluene/triethylamine (3:1, 30 mL) was purged with nitrogen for 15 min. To this solution,  $\text{AsPh}_3$  (4 mg, 0.001 mmol) and  $\text{Pd}_2(\text{dba})_3$  (1 mg, 0.001 mmol) were added and stirred at 35 °C for 15 h. The formation of triad was confirmed by the appearance of new spot on TLC as well as from the characteristic splitting pattern of bands observed in UV–vis spectroscopy. The crude compound was purified by silica gel column chromatography and the triad **9** was collected using petroleum ether/dichloromethane (20:70) as a purple solid (18 mg, 58%). Mp >300 °C. IR (KBr film):  $\nu$ =3055, 2922, 2872, 1452, 990, 750  $\text{cm}^{-1}$ .  $^1\text{H}$  NMR (400 MHz,  $\text{CDCl}_3$ , 25 °C):  $\delta$ =−2.64 (s, 2H, NH), −2.72 (s, 1H, NH), 0.38 (s, 9H, Si-CH<sub>3</sub>), 2.72 (s, 15H, Ar-CH<sub>3</sub>), 2.76 (s, 6H, Ar-CH<sub>3</sub>), 7.5–7.54 (m, 12H, Ar), 7.62 (d,  $J$ =8.0 Hz, 4H, Ar), 7.88 (d,  $J$ =8.0 Hz, 4H, Ar), 7.94 (d,  $J$ =7.2 Hz, 8H, Ar), 8.04–8.10 (m, 14H, Ar), 8.12 (d,  $J$ =7.8 Hz, 4H, Ar), 8.17 (d,  $J$ =7.8 Hz, 4H, Ar), 8.20 (d,  $J$ =7.8 Hz, 4H, Ar), 8.60–8.64 (m, 4H,  $\beta$ -pyrrole), 8.66–8.71 (m, 6H,  $\beta$ -pyrrole), 8.76 (d,  $J$ =4.4 Hz, 1H,  $\beta$ -pyrrole), 8.79 (d,  $J$ =4.4 Hz, 2H,  $\beta$ -pyrrole), 8.81 (d,  $J$ =4.4 Hz, 2H,  $\beta$ -pyrrole), 8.84–8.88 (m, 5H,  $\beta$ -pyrrole), 8.92–8.96 (m, 2H,  $\beta$ -pyrrole), 9.68 (d,  $J$ =4.6 Hz, 1H,  $\beta$ -thiophene), 9.77 (d,  $J$ =4.6 Hz, 1H,  $\beta$ -thiophene) ppm.  $^{13}\text{C}$  NMR (100 MHz,  $\text{CDCl}_3$ , 25 °C):  $\delta$ =21.4, 21.6, 22.2, 29.7, 93.6, 96.0, 126.2, 127.4, 127.6, 128.3, 131.2, 134.4, 136.0, 137.5, 139.2, 143.8, 144.7, 149.9, 150.9, 152.7, 157.8, 159.9 ppm. ES-MS:  $\text{C}_{146}\text{H}_{101}\text{N}_{11}\text{SSiZn}$ , calcd av mass 2135.0, obsd  $m/z$  2134.8 [ $\text{M}^+$ , 60%].

#### 4.1.5. $\text{ZnN}_4\text{-N}_4\text{-N}_3\text{S}$ porphyrin triad **10**

The triad **10** was obtained by treating 1 equiv porphyrin triad **9** (20 mg, 0.0093 mmol) with 10 equiv of  $\text{K}_2\text{CO}_3$  (12.8 mg, 0.093 mmol) in THF/ $\text{CH}_3\text{OH}$  under refluxing condition. The solvent was removed on rotary evaporator under vacuum and obtained triad **10** as a purple solid (16 mg, 82%). Mp >300 °C. IR (KBr film):  $\nu$ =3310, 3055, 2922, 2872, 1452, 990, 750  $\text{cm}^{-1}$ .  $^1\text{H}$  NMR (400 MHz,  $\text{CDCl}_3$ , 25 °C):  $\delta$ =−2.65 (s, 2H, NH), −2.72 (s, 1H, NH), 3.20 (s, 1H, CCH), 2.72 (s, 15H, Ar-CH<sub>3</sub>), 2.76 (s, 6H, Ar-CH<sub>3</sub>), 7.5–7.54 (m, 12H, Ar), 7.62 (d,  $J$ =8.0 Hz, 4H, Ar), 7.88 (d,  $J$ =8.0 Hz, 4H, Ar), 7.94 (d,  $J$ =7.2 Hz, 8H, Ar), 8.04–8.10 (m, 14H, Ar), 8.12 (d,  $J$ =7.8 Hz, 4H, Ar), 8.17 (d,  $J$ =7.8 Hz, 4H, Ar), 8.20 (d,  $J$ =7.8 Hz, 4H, Ar), 8.60–8.64 (m, 4H,  $\beta$ -pyrrole), 8.66–8.71 (m, 6H,  $\beta$ -pyrrole), 8.76 (d,  $J$ =4.4 Hz, 1H,  $\beta$ -pyrrole), 8.79 (d,  $J$ =4.4 Hz, 2H,  $\beta$ -pyrrole), 8.81 (d,  $J$ =4.4 Hz, 2H,  $\beta$ -pyrrole), 8.84–8.88 (m, 5H,  $\beta$ -pyrrole), 8.92–8.96 (m, 2H,  $\beta$ -pyrrole), 9.68 (d,  $J$ =4.6 Hz, 1H,  $\beta$ -thiophene), 9.77 (d,  $J$ =4.6 Hz, 1H,  $\beta$ -thiophene) ppm.  $^{13}\text{C}$  NMR (100 MHz,  $\text{CDCl}_3$ , 25 °C):  $\delta$ =21.4, 21.6, 22.2, 29.7, 93.6, 96.0, 126.2, 127.4, 127.6, 128.3, 131.2, 134.4, 136.0, 137.5, 139.2, 143.8, 144.7, 149.9, 150.9, 152.7, 157.8, 159.9 ppm. ES-MS:  $\text{C}_{143}\text{H}_{93}\text{N}_{11}\text{S}_2\text{Zn}$ , calcd av mass 2062.8, obsd  $m/z$  2062.7 [ $\text{M}^+$ , 50%].

#### 4.1.6. $\text{ZnN}_4\text{-N}_4\text{-N}_3\text{S-N}_2\text{S}_2$ porphyrin tetrad **2**

A solution of triad **10** (15 mg, 0.007 mmol) and **6** (7 mg, 0.007 mmol) in dry toluene/triethylamine (3:1, 30 mL) was purged with nitrogen for 15 min. To this solution,  $\text{AsPh}_3$  (7 mg, 0.001 mmol) and  $\text{Pd}_2(\text{dba})_3$  (3 mg, 0.001 mmol) were added and stirred at 35 °C for 15 h. The formation of tetrad was confirmed by the appearance of new spot on TLC as well as from the characteristic splitting pattern of bands observed in UV–vis spectroscopy. The crude compound was purified by silica gel column chromatography and the desired tetrad **2** was collected using dichloromethane as a purple solid (5 mg, 31%). Mp >300 °C. IR (KBr film):  $\nu$ =3054, 2922, 2858, 1452, 992, 754  $\text{cm}^{-1}$ .  $^1\text{H}$  NMR (400 MHz,  $\text{CDCl}_3$ , 25 °C):  $\delta$ =−2.65 (s, 2H, NH), −2.82 (s, 1H, NH), 2.74 (s, 27H, Ar-CH<sub>3</sub>), 7.52 (d,  $J$ =8.0 Hz, 14H, Ar), 7.60 (d,  $J$ =8.0 Hz, 12H, Ar), 7.87 (d,  $J$ =7.6 Hz, 2H, Ar), 7.92–7.98 (m, 6H, Ar), 8.06 (d,  $J$ =8.0 Hz, 12H, Ar), 8.09–8.14 (m, 12H, Ar), 8.20 (d,  $J$ =8.0 Hz, 6H, Ar), 8.61–8.64 (m, 8H,  $\beta$ -pyrrole), 8.68–8.72 (m, 7H,  $\beta$ -pyrrole), 8.74 (d,  $J$ =4.4 Hz, 1H,  $\beta$ -pyrrole), 8.78 (d,  $J$ =4.4 Hz, 1H,  $\beta$ -pyrrole), 8.78 (d,  $J$ =4.4 Hz, 2H,  $\beta$ -pyrrole),

8.84–8.88 (m, 3H,  $\beta$ -pyrrole), 8.95 (m, 4H,  $\beta$ -pyrrole), 9.60 (d,  $J=5.2$  Hz, 1H,  $\beta$ -thiophene), 9.66–9.72 (m, 3H,  $\beta$ -thiophene), 9.76 (d,  $J=5.2$  Hz, 2H,  $\beta$ -thiophene) ppm.  $^{13}\text{C}$  NMR (100 MHz,  $\text{CDCl}_3$ , 25 °C):  $\delta=21.4$ , 31.4, 81.8, 91.0, 123.9, 127.3, 127.4, 128.2, 128.9, 131.3, 132.6, 134.1, 134.3, 135.7, 136.5, 137.5, 137.9, 139.1, 141.1, 144.1, 147.3, 152.7, 154.5 ppm. ES-MS:  $\text{C}_{190}\text{H}_{126}\text{N}_{13}\text{S}_3\text{Zn}$ , calcd av mass 2752.4, obsd  $m/z$  2752.1 [ $\text{M}^+$ , 25%].

## Acknowledgements

M.R. thanks BRNS and CSIR for financial support. Thanks are also to Ms. Smita Rai for her help in preparing the manuscript.

## References and notes

- Burrell, A. K.; Officer, D. L.; Plieger, P. G.; Reid, D. C. W. *Chem. Rev.* **2001**, *101*, 2751–2796.
- Suslick, K. S.; Rakow, N. A.; Kosal, M. E.; Chou, J.-H. *J. Porphyrins Pthalocyanines* **2000**, *4*, 407–413.
- Holten, D. F.; Bocian, D. F.; Lindsey, J. S. *Acc. Chem. Res.* **2002**, *35*, 57–69.
- Dongho, K.; Osuka, A. *Acc. Chem. Res.* **2004**, *37*, 735–745.
- Naoki, A.; Osuka, A.; Cho, H.-S.; Dongho, K. *J. Photochem. Photobiol., C* **2002**, *3*, 25–52.
- Gust, D.; Moore, T. A.; Moore, A. L. *Acc. Chem. Res.* **2001**, *34*, 40–48.
- Hsiao, J.-S.; Kruegar, B. P.; Wagner, R. W.; Johnson, T. E.; Delaney, J. K.; Mauzerall, D. C.; Fleming, G. R.; Lindsey, J. S.; Bocian, D. F.; Donohoe, R. J. *J. Am. Chem. Soc.* **1996**, *118*, 11181–11193.
- Yang, S. I.; Laxmi, R. K.; Seth, J.; Riggs, J. A.; Arai, T.; Kim, D.; Bocian, D. F.; Holten, D.; Lindsey, J. S. *J. Phys. Chem. B* **1998**, *102*, 9426–9436.
- Lammi, R. K.; Ambrose, A.; Balasubramanian, T.; Wagner, R. W.; Bocian, D. F.; Holten, D.; Lindsey, J. S. *J. Am. Chem. Soc.* **2000**, *122*, 7579–7591.
- del Rosario Benites, M.; Johnson, T. E.; Weghorn, S.; Yu, L.; Rao, P. D.; Diers, J. R.; Yang, S. I.; Kirmaier, C.; Bocian, D. F.; Holten, D.; Lindsey, J. S. *J. Mater. Chem.* **2002**, *12*, 65–80.
- Wagner, R. W.; Johnson, T. E.; Li, F.; Lindsey, J. S. *J. Org. Chem.* **1995**, *60*, 5266–5273.
- Prathapan, S.; Johnson, T. E.; Lindsey, J. S. *J. Am. Chem. Soc.* **1993**, *115*, 7519–7520.
- Wagner, R. W.; Lindsey, J. S. *J. Am. Chem. Soc.* **1994**, *116*, 9759–9760.
- Ambrose, A.; Kirmaier, C.; Wagner, R. W.; Loewe, R. S.; Bocian, D. F.; Holten, D.; Lindsey, J. S. *J. Org. Chem.* **2002**, *67*, 3811–3826.
- Wagner, R. W.; Lindsey, J. S.; Seth, J.; Palaniappan, V.; Bocian, D. F. *J. Am. Chem. Soc.* **1996**, *118*, 3996–3997.
- Gupta, I.; Ravikanth, M. *J. Org. Chem.* **2004**, *69*, 6796–6811.
- Punidha, S.; Agarwal, N.; Ravikanth, M. *Eur. J. Org. Chem.* **2005**, 2500–2517.
- Punidha, S.; Ravikanth, M. *Synlett* **2005**, 2199–2203.
- Rai, S.; Ravikanth, M. *Tetrahedron* **2007**, *63*, 2455–2465.
- Gupta, I.; Ravikanth, M. *Inorg. Chim. Acta* **2007**, *360*, 1731–1742.
- Punidha, S.; Agarwal, N.; Gupta, I.; Ravikanth, M. *Eur. J. Org. Chem.* **2007**, 1168–1175.
- Cho, W.-S.; Kim, H.-J.; Littler, B. J.; Miller, M. A.; Lee, C.-H.; Lindsey, J. S. *J. Org. Chem.* **1999**, *64*, 7890–7901.
- Ames, D. E.; Bull, D.; Takundwa, C. *Synthesis* **1981**, 364–365.
- Farina, V.; Krishnan, B. *J. Am. Chem. Soc.* **1991**, *113*, 9585–9595.
- Latos-Grazynski, L. In *The Porphyrin Handbook*; Kadish, K. M., Smith, K. M., Guillard, R., Eds.; Academic: New York, NY, 2000; Vol. 2, pp 361–416.
- Pandian, R. P.; Chandrashekar, T. K. *Inorg. Chem.* **1994**, *33*, 3317–3324.